Journal of Applied Polymer Science

Torrefied Biomass-Polypropylene Composites

Bor-Sen Chiou,[1] Diana Valenzuela-Medina,[1] Mark Wechsler,[2] Cristina Bilbao-Sainz,[1] Artur K. Klamczynski,[1] Tina G. Williams,[1] Delilah F. Wood,[1] Greg M. Glenn,[1] William J. Orts[1]

[1]Bioproduct Chemistry and Engineering, US Department of Agriculture, Albany, California 94710

[2]Renewable Fuel Technologies, San Mateo, California 94403

Correspondence to: B. Chiou (E-mail: bor-sen.chiou@ars.usda.gov)

ABSTRACT: Torrefied almond shells and wood chips were incorporated into polypropylene as fillers to produce torrefied biomass-polymer composites. The composites were prepared by extrusion and injection molding. Response surface methodology was used to examine the effects of filler concentration, filler size, and lignin factor (relative lignin to cellulose concentration) on the material properties of the composites. The heat distortion temperatures, thermal properties, and tensile properties of the composites were characterized by thermomechanical analysis, differential scanning calorimetry, and tensile tests, respectively. The torrefied biomass composites had heat distortion temperatures of 8–24°C higher than that of neat polypropylene. This was due to the torrefied biomass restricting mobility of polypropylene chains, leading to higher temperatures for deformation. The incorporation of torrefied biomass generally resulted in an increase in glass transition temperature, but did not affect melting temperature. Also, the composites had lower tensile strength and elongation at break values than those of neat polypropylene, indicating weak adhesion between torrefied biomass and polypropylene. However, scanning electron microscopy results did indicate some adhesion between torrefied biomass and polypropylene. © 2014 Wiley Periodicals, Inc. J. Appl. Polym. Sci. **2015**, *132*, 41582.

KEYWORDS: cellulose and other wood products; composites; properties and characterization; thermoplastics

Received 18 April 2014; accepted 1 October 2014

DOI: 10.1002/app.41582

INTRODUCTION

Torrefaction of biomass involves heating the sample under inert atmosphere at temperatures between 200 and 300°C for 1 h or less. This removes most moisture and volatile components to produce a fuel comparable to low-rank coal. Torrefaction had mostly been examined as a method to produce high density fuel as a drop-in replacement for coal. In this application, torrefied biomass can lose up to half of its initial mass, but still retains 70–90% of its energy value. Torrefaction had also been examined as a pretreatment method for gasification.[1,2] In this case, torrefied biomass has a lower oxygen/carbon ratio and moisture content than raw biomass, leading to more efficient gasification.

Although torrefied biomass had been examined as a high density fuel source, little research had been performed on using torrefied biomass as filler in polymer composites. Torrefied biomass has several advantages over natural fillers currently in use, such as wood flour and natural fibers. One is that it is more hydrophobic, since the hydrophilic hemicellulose and cellulose components degrade to some extent during torrefaction.[3–5] This should improve its dispersion and compatibility in a polymer matrix compared to raw biomass. Shoulaifar et al.[6] examined the increase in hydrophobicity of torrefied spruce wood by determining carboxylic acid group concentrations in raw and torrefied samples. Carboxylic acid groups accounted for some of the hygroscopic nature of wood. They found that carboxylic acid concentrations decreased at higher torrefaction temperatures. In addition, Felfi et al.[7] immersed raw and torrefied wood briquettes in water. They found that raw briquettes disintegrated, but torrefied briquettes remained intact even after 17 days. Another advantage of torrefied biomass over wood flour and natural fibers is their low moisture content.[8,9] Torrefied biomass has equilibrium moisture contents of 2–4% under ambient conditions, which should result in better moisture resistance properties of torrefied biomass composites compared to wood-polymer composites. Also, the low moisture content of torrefied biomass should provide more resistance to microbial attack than raw biomass. For instance, Medic et al.[9] found that raw corn stover stored at 30°C and 97% relative humidity for 30 days lost 17% of its mass. In comparison, samples torrefied at 200, 250, and 300°C lost 6%, <1%, and <1% of their masses, respectively. The authors speculated that torrefied samples might have contained lignin degradation products, such as furan and phenol derivatives, which might be toxic to microorganisms.

Table I. Box–Behnken Design with Uncoded Independent Variable Values and Experimental Results

Run	Filler concentration (% w/w)	Lignin factor	Filler size (μm)	T_d (°C)	T_g (°C)	T_m (°C)	Tensile modulus (MPa)	Tensile strength (MPa)	Elongation at break (%)
1	12.5	0.56	854	152.9 ± 1.9	−7.3 ± 2.8	166.2 ± 0.4	922.4 ± 44.2	21.9 ± 2.2	6.1 ± 0.8
2	20	0.49	854	148.1 ± 5.2	−11.0 ± 1.5	166.3 ± 0.5	918.6 ± 35.3	20.6 ± 1.2	6.2 ± 1.3
3	12.5	0.63	1545	151.8 ± 5.1	−12.1 ± 1.3	166.8 ± 0.5	828.2 ± 36.2	22.1 ± 1.5	7.8 ± 1.1
4	12.5	0.56	854	147.6 ± 1.2	−7.6 ± 0.4	166.3 ± 0.4	932.5 ± 52.3	22.8 ± 2.8	6.6 ± 1.1
5	20	0.63	854	149.5 ± 3.9	−8.6 ± 3.4	166.8 ± 0.6	943.7 ± 37.7	22.3 ± 0.5	6.6 ± 0.4
6	12.5	0.49	163	149.6 ± 4.1	−8.9 ± 6.2	166.0 ± 0.5	968.3 ± 70.9	27.0 ± 0.8	8.9 ± 0.2
7	20	0.56	163	157.1 ± 2.6	−12.2 ± 1.4	166.1 ± 1.3	917.2 ± 63.7	23.2 ± 0.6	8.1 ± 0.2
8	5	0.56	163	152.5 ± 3.9	−12.7 ± 1.1	166.9 ± 0.4	943.5 ± 70.6	29.3 ± 1.1	11.8 ± 0.3
9	5	0.63	854	149.5 ± 2.1	−13.4 ± 0.4	167.1 ± 1.1	848.4 ± 59.2	27.0 ± 1.5	9.8 ± 1.5
10	12.5	0.63	163	151.7 ± 7.1	−15.0 ± 0.7	166.3 ± 0.3	934.9 ± 40.8	26.7 ± 0.4	9.7 ± 0.3
11	12.5	0.56	854	148.5 ± 6.1	−12.6 ± 3.4	166.4 ± 0.6	840.9 ± 31.3	21.7 ± 1.7	7.6 ± 1.0
12	12.5	0.49	1545	140.8 ± 10.6	−13.5 ± 1.2	167.1 ± 1.1	1060.2 ± 193.1	26.8 ± 4.8	7.0 ± 0.7
13	5	0.56	1545	146.4 ± 5.0	−12.5 ± 0.7	166.4 ± 0.7	777.3 ± 58.0	23.7 ± 2.8	9.2 ± 1.7
14	20	0.56	1545	153.1 ± 3.9	−14.7 ± 1.1	166.9 ± 0.8	865.8 ± 62.5	21.0 ± 2.5	6.9 ± 1.0
15	5	0.49	854	146.2 ± 2.4	−11.5 ± 1.8	167.2 ± 0.7	945.1 ± 55.3	28.1 ± 0.9	9.5 ± 1.0
16	0	—	—	132.8 ± 2.8	−13.4 ± 2.5	167.5 ± 0.3	908.5 ± 43.7	36.2 ± 1.7	714.6 ± 39.4

The experimental results for neat polypropylene are also included for comparison.

There had been several studies involving the use of bamboo charcoal[10] and corn stover biochar[11] as fillers in polymer composites. Charcoal and biochar are produced at much higher temperatures than those used to produce torrefied biomass. Guo et al.[10] found that incorporating bamboo charcoal into poly(ethylene terephthalate) improved its thermal stability. Peterson[11] determined that carboxylated styrene-butadiene composites containing low concentrations of corn stover biochar (10% (w/w)) exhibited improved tensile properties.

There had also been few studies examining almond shells as fillers in composites. Currently, almond shells are burned directly as fuel. In one study involving almond shells, Essabir et al.[12] incorporated almond shells into polypropylene using a twin-screw extruder. The authors found that an increase in almond shell concentration resulted in an increase in tensile modulus, but a decrease in tensile strength and strain at yield.

In this study, we incorporated torrefied almond shells and wood chips into polypropylene to produce torrefied biomass-polymer composites. We used a Box–Behnken design and response surface methodology to examine the effects of filler size, filler concentration, and lignin factor on the material properties of the composites. We used thermomechanical analysis (TMA), differential scanning calorimetry (DSC), and tensile tests to examine the heat distortion temperatures, thermal properties, and tensile properties of the composites, respectively. We also used scanning electron microscopy (SEM) to examine interactions between filler and polymer in the composites.

EXPERIMENTAL

Materials

Polypropylene (Pro-fax PD702) was obtained from Lyondellbasell Industries (Houston, TX). It is a homopolymer with a melt-mass flow rate of 35 g/10 min. Three different torrefied biomass samples were obtained from Renewable Fuel Technologies (San Mateo, CA) and used to make the composites. These were ground almond shells torrefied at 280°C, wood torrefied at 280°C, and ground almond shells torrefied at 300°C. All samples were torrefied for 15 min. These samples were chosen for differences in their lignin contents. The almond shells torrefied at 280°C, wood torrefied at 280°C, and almond shells torrefied at 300°C had lignin factors of 0.49, 0.59, and 0.63, respectively. Lignin factors were determined by Fourier Transform Infra-red (FTIR) spectroscopy and calculated as the ratio of lignin absorbance peaks (1250–1430 cm^{-1}) to cellulose absorbance peak (1030 cm^{-1}). A Nicolet (Waltham, MA) iS4 FTIR spectrometer with iD5 Attenuated Total Reflectance Accessory was used to perform the FTIR experiments. The IR spectrum for each sample was an average of 18 scans with a resolution of 4 cm^{-1}. Each torrefied sample was also ground and sieved to produce particles of different sizes. The particle sizes were between 149 and 177 μm (using 100 and 80 mesh sieves), 841 and 1000 μm (using 20 and 18 mesh sieves), and 1410 and 1680 μm (using 14 and 12 mesh sieves). The particle sizes were designated as the average between the minimum and maximum sizes. Consequently, the sizes were 163, 854, and 1545 μm.

Sample Preparation

A Leistritz (Somerville, NJ) Micro 18 corotating twin-screw extruder was used to prepare the samples. The extruder has six heating zones with the first five cooled by water. The temperatures for each zone were 180, 180, 175, 170, 160, and 150°C from feed to die. The screws have a diameter of 18 mm and the barrel has a length to diameter ratio of 30 : 1.

A Boy Machines (Hauppauge, NY) 15 S injection molder was used to prepare samples for testing. The injection molder has three heated zones, with each zone set at 180°C.

Design of Experiments

Response surface methodology using Minitab (State College, PA) software (version 14.12) was used to determine the effects of three factors, filler concentration, filler size, and lignin factor, on heat distortion temperature, glass transition temperature, melt temperature, tensile modulus, tensile strength, and elongation at break. A Box–Behnken design of three levels and three center points with 15 runs was used for the study. The experiments were performed in triplicate. The filler concentrations were 5, 12.5, and 20% (w/w). The filler sizes were 163, 854, and 1545 μm. The lignin factors were 0.49, 0.59, and 0.63. The details of the design are shown in Table I. All possible regressions were tried and used to obtain the best fit to the response surface. The response surface models were hierarchial, with all models containing the first order terms of filler concentration, filler size, and lignin factor.

Heat Distortion Temperature

A TA Instruments (New Castle, DE) thermomechanical analyzer (TMA 2940) was used to characterize the heat distortion temperature of the samples. The tests were performed according to the ASTM E2092-09 method. Each sample was cut into a rectangular piece with a length of 19 ± 2 mm, a width of 4.9 ± 0.2 mm, and a thickness of 1.56 ± 0.03 mm. Prior to each test, the samples were conditioned in a 50% relative humidity chamber for 48 h. The chamber was maintained at these conditions by using a saturated solution of calcium nitrate tetrahydrate (Fisher Scientific, Philadelphia, PA), $Ca(NO_3)_2{\cdot}4H_2O$, in deionized water. The sample was held at 30°C for one minute and then the temperature was ramped to 170°C at 10°C min^{-1}. The heat distortion temperature was determined at a strain of 2 mm m^{-1}.

Differential Scanning Calorimetry

A TA Instruments (New Castle, DE) differential scanning calorimeter (DSC 2910) was used to measure the thermal properties of the samples. An indium standard was used to calibrate the calorimeter. The sample amount used was 5.0 ± 0.1 mg and each sample was heated from −30°C to 200°C at a rate of 10°C min^{-1}. The sample chamber was purged with nitrogen gas at a flow rate of 75 cm^3 min^{-1}.

Tensile Tests

An Instron (Canton, MA) 5500R universal testing machine was used to measure the tensile properties of the samples. The tests were performed according to the ASTM D638-10 method. Prior to each test, the samples were conditioned in a 50% relative humidity chamber for 48 h. A 1 kN load cell was used and the extension rate was set at 20 mm min^{-1}. At least five replicates were tested for each sample.

Scanning Electron Microscopy

A Hitachi (Pleasanton, CA) S-4700 scanning electron microscope was used to observe the cross-section of the composite's fracture surface after completion of the tensile tests. The voltage was set to 2.0 kV and the current was set to 10 μA. A Denton (Moorestown, NJ) Desk II sputter coater was used to apply a gold/palladium coating to the samples that were affixed to stubs. The samples were sputter coated for 45 s with the

Table II. Coefficients for Response Surface Models

Response	Constant	Variables									R^{2a}
		FC[b]	LF[c]	FS[d]	FC^2	LF^2	FS^2	FC*LF	FC*FS	LF*FS	
T_d (°C)[e]	−21.0	0.2**	622.7**	-2.9×10^{-2}**	—	−562.7*	—	—	—	4.6×10^{-2}**	0.76
T_g (°C)[f]	20.1	−0.5	−66.2**	-1.3×10^{-2}	-2.2×10^{-2}	—	-5.2×10^{-6}**	2.1	—	3.9×10^{-2}*	0.63
T_m (°C)[g]	184.8	−0.4*	−60.4**	1.3×10^{-3}	5.1×10^{-3}**	53.8**	—	0.3	6.3×10^{-5}*	-3.1×10^{-3}	0.84
Tensile modulus (MPa)	3907.9	−22.3	−10327.9*	0.5	−0.5	8819.5*	—	58	5.5×10^{-3}	−1.0**	0.77
Tensile strength (MPa)	143.0	−0.5*	−404.3*	2.6×10^{-3}	—	371.3*	3.4×10^{-6}*	—	1.6×10^{-4}	-2.3×10^{-2}	0.91
Elongation at break (%)	33.0	−0.7*	−65.4	-6.8×10^{-3}*	1.7×10^{-2}*	62.1	2.7×10^{-6}*	—	6.8×10^{-5}	—	0.97

[a] R^2 = coefficient of multiple correlation.
[b] FC = filler concentration.
[c] LF = lignin factor.
[d] FS = filler size.
[e] T_d = heat distortion temperature.
[f] T_g = glass transition temperature.
[g] T_m = melting temperature.
*P (P value) ≤ 0.05; **$P < 0.10$.

discharge current set at 20–30 mA. The vacuum chamber was lowered to a pressure of <100 mTorr.

RESULTS AND DISCUSSION

Heat Distortion Temperature

All composites had larger heat distortion temperatures than that of neat polypropylene, with temperature increases ranging from 8 to 24°C. This is shown in Table I. The response surface model for heat distortion temperature of the composites is shown in Table II. All terms in the response surface model were significant ($P < 0.10$) and the model had an R^2 value of 0.76, indicating a fairly good fit to the data. Figure 1 shows the surface plots of heat distortion temperature as a function of filler size and lignin factor at each filler concentration. Previous studies on biomass-filled polypropylene composites also showed higher heat distortion temperatures compared to neat polypropylene.[13–23] The increase in heat distortion temperature can be explained by the fillers restricting mobility of the polymer chains, leading to higher temperatures for deformation.[17,19,20] In fact, studies had shown that composites containing compatibilizers or surface-treated fillers had higher heat distortion temperatures than those without compatibilizers or surface-treated fillers.[14,17,19,20,22,23] This improvement in heat distortion temperature was attributed to enhanced interfacial strength between filler and polymer matrix, resulting in even greater restricted mobility of polymer chains. Also, most studies had

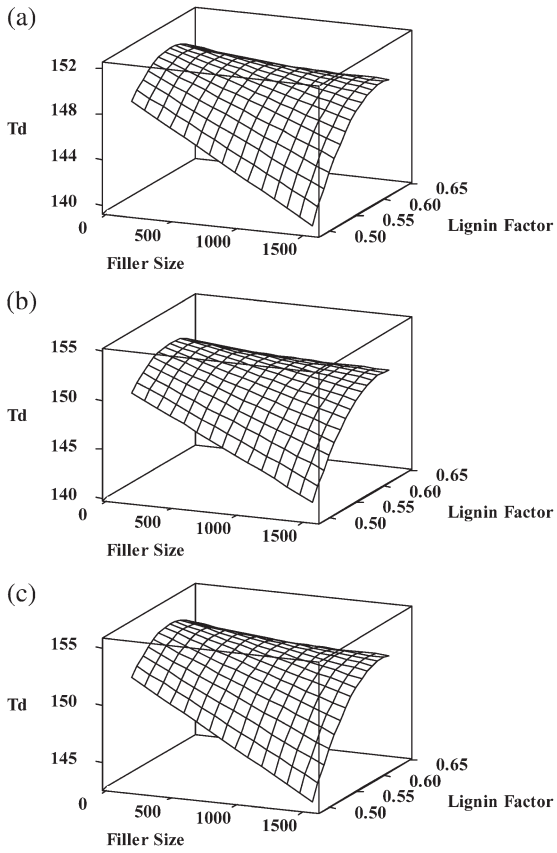

Figure 1. Surface plots of heat distortion temperature (T_d, °C) as a function of filler size (μm) and lignin factor for filler concentrations of (a) 5% (w/w), (b) 12.5% (w/w), and (c) 20% (w/w).

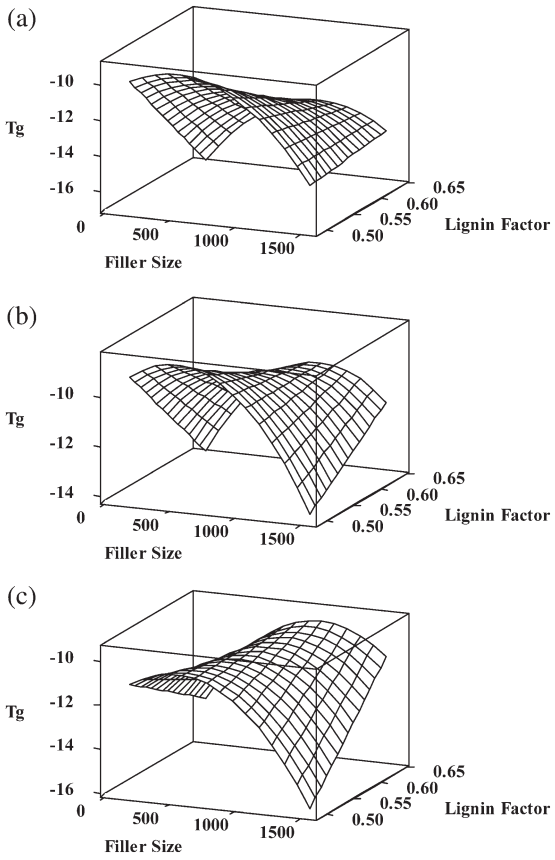

Figure 2. Surface plots of glass transition temperature (T_g, °C) as a function of filler size (μm) and lignin factor for filler concentrations of (a) 5% (w/w), (b) 12.5% (w/w), and (c) 20% (w/w).

shown that an increase in filler concentration led to an increase in heat distortion temperature of the sample.[14–20,22,23] This was consistent with our results, where the regression coefficient of the filler concentration term in the response surface model had a positive sign (see Table II). In addition, there had been few studies examining the effects of filler size on heat distortion temperature. In one study, Sobcyak et al.[23] showed that samples containing larger spruce wood fillers had slightly higher heat distortion temperatures than those with smaller fillers. This was opposite to our results, where we found samples with smaller filler sizes had higher heat distortion temperatures (see Figure 1). These differences might be due to the different filler concentrations and materials used in both studies, resulting in different interactions between filler and matrix. Also, composites with larger lignin factors had higher heat distortion temperatures (see Figure 1). This might be due to increased interactions between the more hydrophobic torrefied fillers with larger lignin factors and polypropylene. These interactions should result in greater restricted mobility of polypropylene chains and a subsequent increase in heat distortion temperature.

Thermal Properties

The composites generally had higher glass transition temperatures than that of neat polypropylene. These temperatures varied from −15 to −7.3°C, compared to −13.4°C for neat polypropylene. This is shown in Table I. The response surface

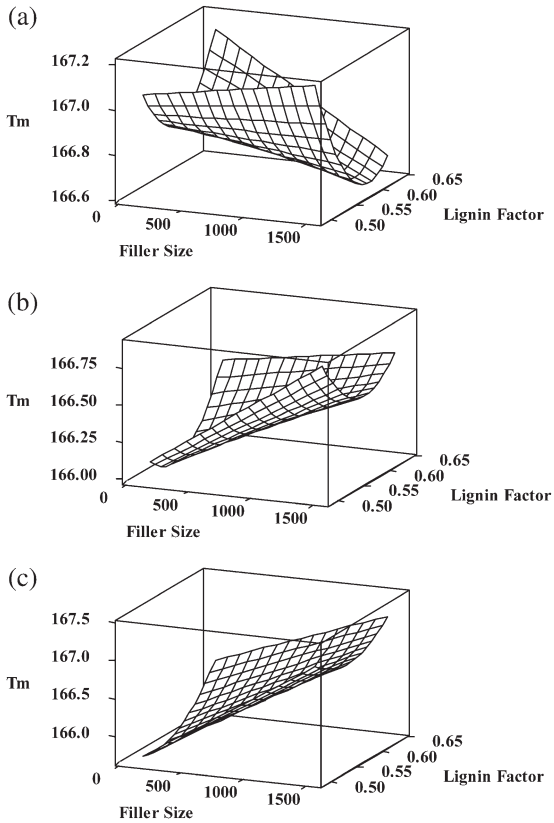

Figure 3. Surface plots of melt temperature (T_m, °C) as a function of filler size (μm) and lignin factor for filler concentrations of (a) 5% (w/w), (b) 12.5% (w/w), and (c) 20% (w/w).

model is shown in Table II and the surface plots of glass transition temperature are shown in Figure 2. The significant terms ($P < 0.10$) in the model included lignin factor, filler size × filler size, and lignin factor × filler size. The filler concentration, filler size, and filler concentration × filler concentration terms were not significant. However, these were included in the model since the all possible regressions method (see Design of Experiments section) determined this model to be the best fit to the data. Omission of these terms would have resulted in a poorer fit to the data. Previous studies had found that incorporating fillers into polymer matrices had resulted in increases in glass transition temperature,[15,21,24–26] consistent with results from this study. This increase was due to interactions between the filler and matrix that reduced polymer chain mobility.

All composites had comparable melt temperatures to neat polypropylene, indicating the fillers had little effect on crystallization behavior of polypropylene. This is shown in Table I. The response surface model is shown in Table II and the surface plots of melt temperature are shown in Figure 3. A previous study[27] also showed that adding wheat straw residue to polypropylene/polyethylene blends did not affect their melt temperatures.

Tensile Properties

The composites generally had larger modulus values than that of neat polypropylene. This is shown in Table I. The response surface model is shown in Table II and the surface plots of tensile modulus are shown in Figure 4. The response surface model

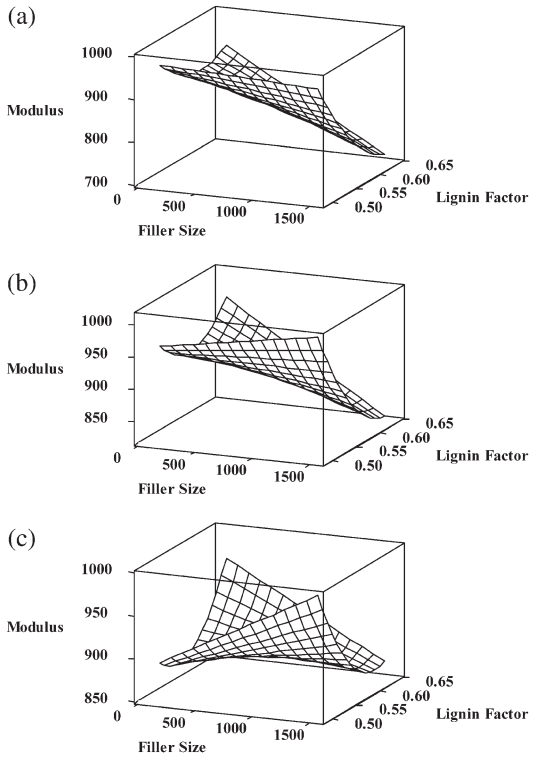

Figure 4. Surface plots of tensile modulus (MPa) as a function of filler size (μm) and lignin factor for filler concentration of (a) 5% (w/w), (b) 12.5% (w/w), and (c) 20% (w/w).

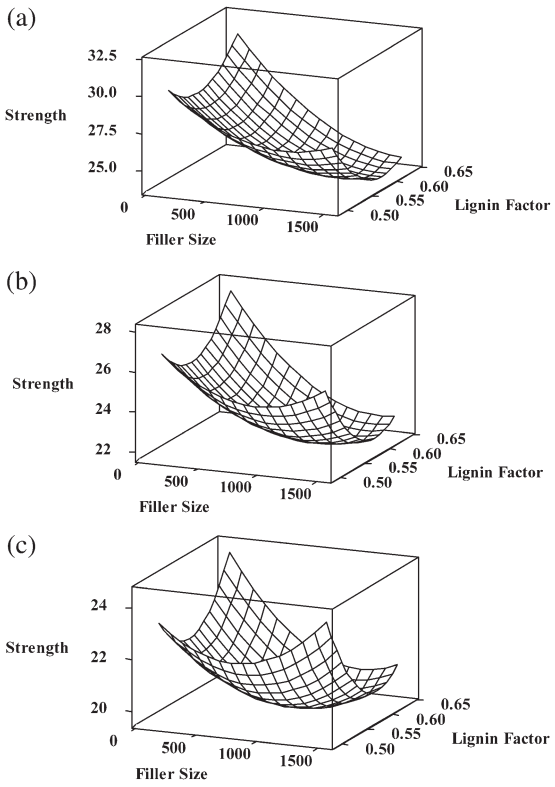

Figure 5. Surface plots of tensile strength (MPa) as a function of filler size (μm) and lignin factor for filler concentrations of (a) 5% (w/w), (b) 12.5% (w/w), and (c) 20% (w/w).

had an R^2 value of 0.77, indicating fairly good fit to the data. The addition of fillers generally had less of an effect on modulus than other tensile properties, such as strength and elongation at break, since modulus values are less sensitive to filler-matrix interactions.[28] Previous studies had generally found an increase in filler concentration resulted in an increase in modulus values.[12,15,17–21,23,27,29–31] This was consistent with results from this study (see Table I). Also, previous studies had determined that an increase in filler size had generally resulted in composites with lower modulus values.[23,30,32,33] This was also consistent with our results (see Figure 4). However, other studies had shown that an increase in filler size resulted in composites with greater modulus values[25,34] or a maximum in modulus value.[31] There had been few studies examining the effects of the filler's lignin content on tensile properties of composites. In one study, Le Digabel et al.[24] incorporated wheat straw fractions containing different lignin contents into polybutylene adipate-*co*-terephthalate. The authors found that composites containing fillers with low lignin contents had higher modulus values. They attributed this result to the higher cellulose contents found in the fillers with low lignin contents.

All composites had lower tensile strengths than that of neat polypropylene, indicating weak adhesion between torrefied biomass and polypropylene. This is shown in Table I. The response surface model is shown in Table II and the surface plots of tensile strength are shown in Figure 5. The response surface model had an R^2 value of 0.91, indicating a very good fit to the model.

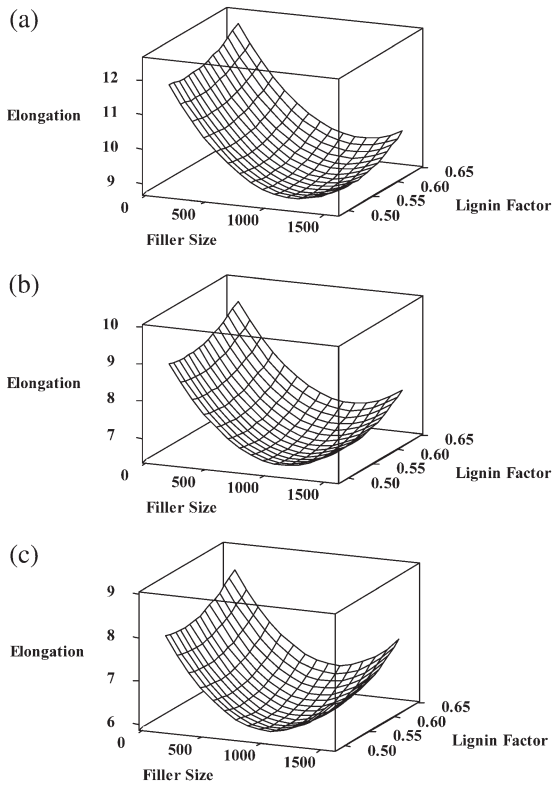

Figure 6. Surface plots of elongation at break (%) as a function of filler size (μm) and lignin factor for filler concentration of (a) 5% (w/w), (b) 12.5% (w/w), and (c) 20% (w/w).

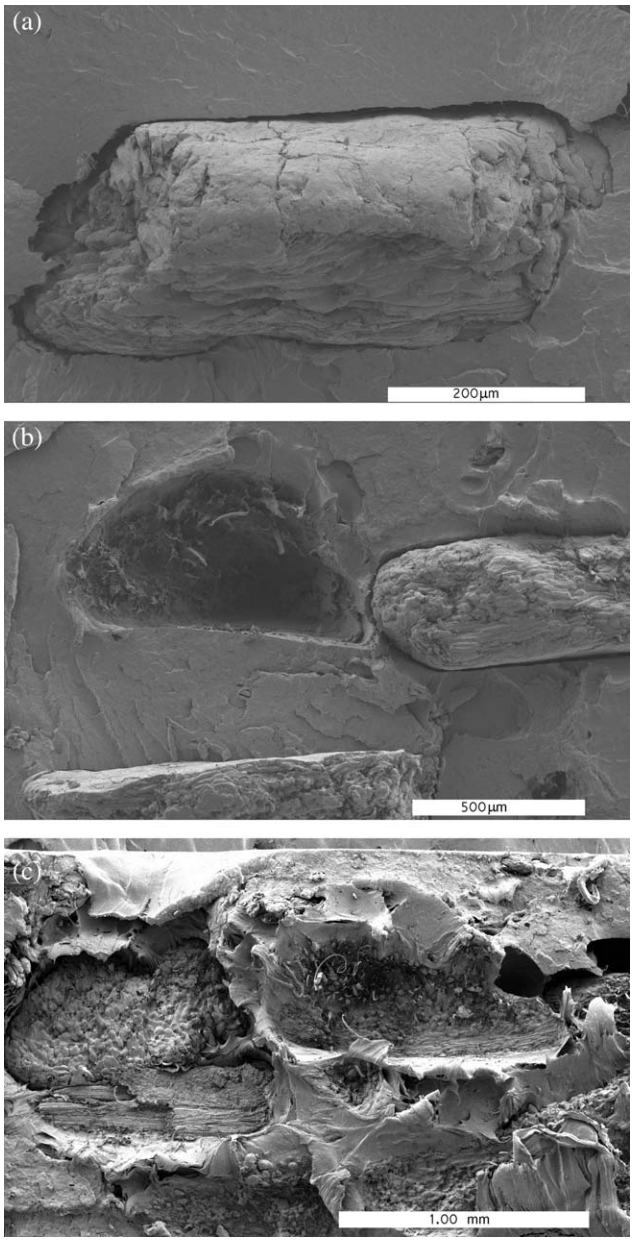

Figure 7. SEM micrographs of samples from (a) run 9 [5% (w/w) almond shells torrefied at 300°C], (b) run 15 [5% (w/w) almond shells torrefied at 280°C], and (c) run 1 [12.5% (w/w) wood torrefied at 280°C].

Previous studies had found that addition of fillers reduced tensile strength of the composites to below that of the neat polymer matrix.[12–14,16,18,21,30,31,34–36] This was due to the fillers not being able to support stress transfer from the matrix. This can usually be addressed by using coupling agents that improve adhesion between filler and matrix, which leads to greater tensile strengths. Previous studies showed that an increase in filler concentration resulted in a decrease in tensile strength of composites.[12,14,16–18,21,23,29–31,34–36] These results were consistent with those in our study (see Figure 5). Also, previous studies had shown that an increase in filler size resulted in composites with lower tensile strengths,[23,25,30,32–34] which was also consistent with our results (see Figure 5). In addition, Le Digabel

et al.[24] found that polymer composites containing fillers with different lignin contents had comparable tensile strengths.

The addition of torrefied biomass to polypropylene resulted in large decreases in elongation at break values. This also indicated weak adhesion between torrefied biomass and polypropylene. This weak adhesion caused debonding to occur at the interface between filler and polymer matrix, which resulted in failure at low elongation values. The elongation at break values of the composites are shown in Table I. The response surface model is shown in Table II and the surface plots of elongation at break are shown in Figure 6. The response surface model had an R^2 value of 0.97, indicating very good fit to the data. Previous studies had shown that addition of fillers generally resulted in composites with lower elongation at break values than that of neat polypropylene.[13,14,16–18,21,29,30,35] Also, an increase in filler concentration led to a further decrease in elongation at break values.[14,16–18,21,27,29,30,35] In addition, previous studies[25,35] found that an increase in filler size resulted in a decrease in elongation at break values. Le Digabel et al.[24] also found that composites containing fillers with high lignin contents generally had higher elongation at break values. These results were all consistent with those found in this study (see Figure 6).

Scanning Electron Microscopy

Many samples showed some space between the torrefied filler particles and the polypropylene matrix, indicating weak interfacial bonding. This was consistent with the tensile property results. One example is shown in Figure 7(a) for the composite from run 9, which contained almond shell particles. Samples also showed holes where the fillers had been pulled from the matrix during tensile tests. This is shown in Figure 7(b,c) for samples containing almond shell (run 15) and wood particles (run 1), respectively. A previous study[37] had shown that debonding of fillers was the dominant deformation mechanism for composites containing large particles with low aspect ratios. Although these results indicated that the filler–matrix interface appeared to be weak, there seemed to be some adhesion between filler and matrix. This was shown by the strands of polypropylene inside the holes [see Figure 7(b,c)], indicating that polypropylene had adhered to the filler surface as the filler was being pulled out.

CONCLUSIONS

The addition of torrefied biomass to polypropylene improved heat distortion temperatures by 8 to 24°C. This was attributed to the fillers restricting mobility of the polymer chains, leading to higher temperatures for deformation. Also, the glass transition temperature of the composites generally increased with incorporation of the torrefied biomass. However, the torrefied biomass did not affect the melt temperature of the composites.

The addition of torrefied biomass generally resulted in greater tensile modulus values of the composites compared to that of neat polypropylene. However, the composites had lower tensile strength and elongation at break values than neat polypropylene. This was due to weak adhesion between torrefied biomass and polypropylene. SEM micrographs showed space between filler and matrix, which was consistent with weak adhesion found from the tensile property measurements. However, there appeared to be some filler–matrix adhesion since some holes left after debonding of fillers contained polypropylene strands.

ACKNOWLEDGMENTS

The authors thank Catherine Davis, Heather Rickansrud, and Gloria Dao for helping with extrusion and characterization of the composites. They also thank Helena Kleiner for performing part of the TGA and DSC analyses.

REFERENCES

1. Prins, M. J.; Ptasinski, K. J.; Janssen, F. J. J. G. *Energy* **2006**, *31*, 3458.
2. Couhert, C.; Salvador, S.; Commandre, J.-M. *Fuel* **2009**, *88*, 2286.
3. Chen, W.-H.; Kuo, P.-C. *Energy* **2011**, *36*, 6451.
4. Chen, W.-H.; Kuo, P.-C. *Energy* **2011**, *36*, 803.
5. Melkior, T.; Jacob, S.; Gerbaud, G.; Hediger, S.; Le Pape, L.; Bonnefois, L.; Bardet, M. *Fuel* **2012**, *92*, 271.
6. Shoulaifar, T. K.; DeMartini, N.; Ivaska, A.; Fardim, P.; Hupa, M. *Bioresource Technol.* **2012**, *123*, 338.
7. Felfli, F. F.; Luengo, C. A.; Suarez, J. A.; Beaton, P. A. *Energy Sustainable Dev.* **2005**, *9*, 19.
8. Achargee, T. C.; Coronella, C. J.; Vasquez, V. R. *Bioresource Technol.* **2011**, *102*, 4849.
9. Medic, D.; Darr, M.; Shah, A.; Rahn, S. *Energy Fuels* **2012**, *26*, 2386.
10. Guo, W.-J.; Su, Y.-Y.; Jhang, J.-L.; Lai, W.-J.; Chen, C.-L.; Cheng, K.-C. *J. Polym. Res.* **2011**, *18*, 1417.
11. Peterson, C. J. *J. Elastom. Plast.* **2012**, *44*, 43.
12. Essabir, E.; Nekhlaoui, S.; Malha, M.; Bensala, M. O.; Arrakhiz, F. Z.; Qaiss, A.; Boufid, R. *Mater. Des.* **2013**, *51*, 225.
13. Zaini, M. J.; Ismail, Z.; Fuad, M. Y. A.; Mustafah, J. *Polym. J.* **1994**, *26*, 637.
14. Kharade, A. Y.; Kale, D. D. *J. Appl. Polym. Sci.* **1999**, *72*, 1321.
15. Bhardwaj, R.; Mohanty, A. K.; Drzal, L. T.; Pourboghrat, F.; Misra, M. *Biomacromolecules* **2006**, *7*, 2044.
16. Ramaraj, B. *J. Appl. Polym. Sci.* **2007**, *103*, 3827.
17. Gonzalez-Sanchez, Z.; Gonzalez-Quesada, M.; de la Orden, M. U.; Martinez Urreaga, J. *J. Appl. Polym. Sci.* **2008**, *110*, 2555.
18. Tasdemir, M.; Biltekin, H.; Caneba, G. T. *J. Appl. Polym. Sci.* **2009**, *112*, 3095.
19. Chattopadhyay, S. K.; Khandal, R. K.; Uppaluri, U.; Ghoshal, A. K. *J. Appl. Polym. Sci.* **2010**, *117*, 1731.
20. Chattopadhyay, S. K.; Khandal, R. K.; Uppaluri, U.; Ghoshal, A. K. *J. Appl. Polym. Sci.* **2011**, *119*, 1619.
21. Gupta, A. K.; Biswal, M.; Mohanty, S.; Nayak, S. K. *Adv. Mech. Eng.* **2012**, *418031*, 13.
22. Shih, Y.-F.; Chen, P.-W.; Wu, C.-S.; Huang, C.-M.; Hsieh, C.-F. *J. Appl. Polym. Sci.* **2012**, *123*, 3046.

23. Sobczak, L.; Lang, R. W.; Reif, M.; Haider, A. *J. Appl. Polym. Sci.* **2013**, *129*, 3687.
24. Le Digabel, F.; Averous, A. *Carbohydr. Polym.* **2006**, *66*, 537.
25. Averous, A.; Le Digabel, F. *Carbohydr. Polym.* **2006**, *66*, 480.
26. Sahoo, S.; Misra, M.; Mohanty, A. K. *J. Appl. Polym. Sci.* **2013**, *127*, 4110.
27. Le Digabel, F.; Boquillon, N.; Dole, P.; Monties, B.; Averous, A. *J. Appl. Polym. Sci.* **2004**, *93*, 428.
28. Kiss, A.; Fekete, E.; Pukanszky, B. *Compos. Sci. Technol.* **2007**, *67*, 1574.
29. Rosch, J.; Mulhaupt, R. *Polym. Bull.* **1994**, *32*, 361.
30. Febrianto, F.; Setyawati, D.; Karina, M.; Bakar, E. S.; Hadi, Y. S. *J. Biol. Sci.* **2006**, *6*, 337.
31. Rimdusit, S.; Smittakorn, W.; Jittarom, S.; Tiptipakorn, S. *Eng. J.* **2011**, *15*, 17.
32. Stark, N. M.; Rowlands, R. E. *Wood Fiber Sci.* **2003**, *35*, 167.
33. Nourbakhsh, A.; Karegarfard, A.; Ashori, A.; Nourbakhsh, A. *J. Thermoplast. Compos. Mater.* **2010**, *23*, 169.
34. Rozman, H. D.; Saad, M. J.; Ishak, Z. A. M. *J. Appl. Polym. Sci.* **2003**, *87*, 827.
35. Zaini, M. J.; Fuad, M. Y. A.; Ismail, Z.; Mansor, M. S.; Mustafah, J. *Polym. Int.* **1996**, *40*, 51.
36. Alexy, P.; Kosikova, B.; Podstranska, G. *Polymer* **2000**, *41*, 4901.
37. Renner, K.; Kenyo, C.; Moczo, J.; Pukanszky, B. *Compos. A* **2010**, *41*, 1653.